PERGAMON

Carbon 40 (2002) 1715–1728

CARBON

Carbon nanotube films as electron field emitters

Jean-Marc Bonard*, Mirko Croci, Christian Klinke, Ralph Kurt[1], Olivier Noury, Nicolas Weiss

Département de Physique, Ecole Polytechnique Fédérale de Lausanne, CH-1015 Lausanne EPFL, Switzerland

Received 3 April 2001; accepted 12 December 2001

Abstract

Carbon nanotubes have been recognized as one of the most promising electron field emitters currently available. We review the state of the art of current research on the electron field emission properties of carbon nanotube films and present recent results outlining their potential as field emitters as well as illustrating some current concerns in the research field.

Keywords: A. Carbon nanotubes; B. Chemical vapor deposition; D. Field emission

1. Introduction

Field emission has emerged as one of the most promising applications for carbon-based films, as attested by the increasing efforts of researchers all over the world. In particular, carbon nanotube emitters are purported to be ideal candidates for the next generation of field emission flat panel displays. Carbon nanotubes [1–7] are very attractive, because they are capable of emitting high currents (up to 1 A/cm^2) at low fields (~5 V/μm), and their potential as emitters in various devices has been amply demonstrated during the last five years [8]. Furthermore, the controlled deposition of nanotubes on a substrate has recently become possible through the combined use of chemical vapor deposition (CVD) methods and catalyst patterning techniques. The challenge now is to develop these exceptional properties to realise viable devices.

Carbon nanotubes can be used as electron sources in two different types of setup, namely single and multiple electron beam devices. One possible application of a single electron beam instrument is an electron microscope that uses a single nanotube as a field emission electron gun to produce a highly coherent electron beam [9]. Conversely, flat panel displays are the most popular example of multiple beam instruments where a continuous or patterned film of nanotubes provides a large number of independent electron sources. We will focus here on the latter embodiment, and review some recent results on the field emission from carbon nanotubes that outline their potential as field emitters as well as illustrate some of the current concerns in the research field. Single electron sources, with related results on the emission mechanism and workfunction, have been extensively reviewed in Refs. [8,10].

2. Field emission

What actually is field emission, and why is it so interesting for some applications? Field emission is the extraction of electrons from a solid by tunneling through the surface potential barrier (for reviews on field emission, see Refs. [11–14]). As shown schematically in Fig. 1, the potential barrier is square when no electric field is present. Its shape becomes triangular when a negative potential is applied to the solid, with a slope that depends on the amplitude of the local electric field F just above the surface. The local electric field is not simply V/d_0, which is the macroscopic field obtained with an applied voltage V between two planar and parallel electrodes separated by a distance d_0. The local field, in most cases, will be higher by a factor β, which gives the aptitude of the emitter to amplify the field and is accordingly termed the field amplification factor. β is determined solely by the

*Corresponding author. Tel.: +41-21-693-4410; fax: +41-21-693-4410.

E-mail addresses: jean-marc.bonard@epfl.ch (J.-M. Bonard), http://ipewww.epfl.ch/nanotubes.html (J.-M. Bonard).

[1]Present address: Philips Research Laboratories Eindhoven, Prof. Holstlaan 4 (WA 03), 5656 AA Eindhoven, The Netherlands.

0008-6223/02/$ – see front matter
PII: S0008-6223(02)00011-8

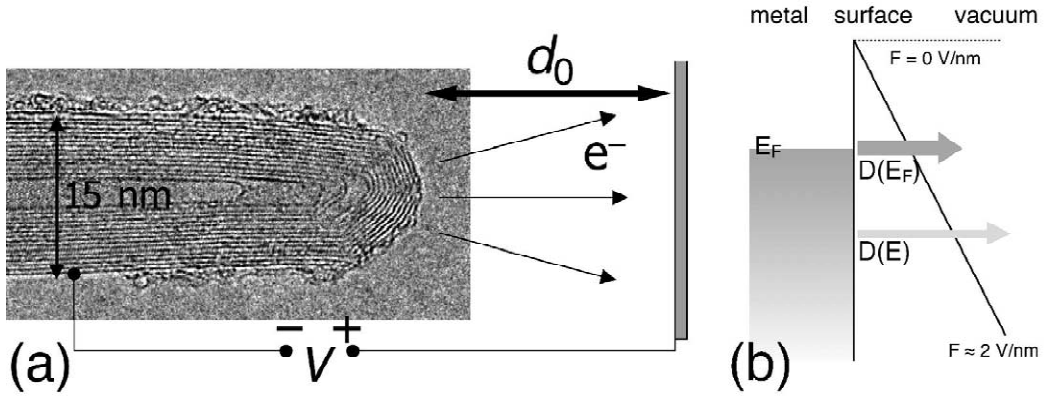

Fig. 1. (a) Schematic of a field emission experiment: a potential is applied between a nanotube (transmission electron microscopy (TEM) micrograph) and a counterelectrode located at a distance d_0. (b) Standard field emission model from a metallic emitter.

geometrical shape of the emitter, and the field at the emitter surface is often written as $F = \beta E = \beta V/d_0$, where E is the macroscopic field. Tunneling through the surface barrier becomes significant when the thickness of the barrier is comparable to the electron wavelength in the solid. Field emission will most likely peak at the Fermi level and is influenced therefore by the workfunction, ϕ, as shown in Fig. 1. In fact, a simple model (the Fowler–Nordheim model) shows that the dependence of the emitted current on the local electric field and the workfunction is exponential-like, with dependence $I \propto (F^2/\phi)\exp(-B\phi^{3/2}/F)$, with $B = 6.83 \times 10^9$ (V eV$^{-3/2}$ m^{-1}). As a consequence, small variations of the shape or surrounding of the emitter (which determine the geometric field enhancement β) and/or the chemical state of the solid or of its surface (which influence the workfunction) have a strong impact on the emitted current. One can also estimate either ϕ or β from measurements, provided that they follow the Fowler–Nordheim model. This can be done with a Fowler–Nordheim plot, i.e. by plotting $\ln(I/V^2)$ versus $1/V$. One should obtain a straight line with a slope that depends on ϕ, β and d_0. For carbon film emitters, ϕ is usually taken as 5 eV.

Note that the Fowler–Nordheim model is valid only for flat surfaces at 0 K, and is in many cases not satisfactory. The model is, however, simple and widely used. One can only hope that efforts that aim to extend the model [15] or to develop numerical approaches [16] will soon supplement it.

Field emitters have several advantages over thermoelectronic emitters. First, the emitter does not have to be heated, which eliminates the need for a heat source or a heating loop. The energy spread of the emitted electrons is also far smaller. Such emitters are easy to realize in microscopic dimensions and to incorporate in emitter arrays, and, finally, the emitted current can be controlled with the applied voltage. It is therefore not surprising that researchers are aiming at replacing thermoelectronic with field emitters in various applications. Displays (with one or several electron sources for each pixel) and microwave tubes are two examples.

3. Fabrication of carbon nanotube film emitters

3.1. Overview

Two basic types of techniques are presently available to produce carbon nanotubes: the vaporization methods (arc discharge, laser ablation) and the catalytic decomposition of hydrocarbons over metal catalysts (also termed CVD methods, for chemical vapor deposition).

Arc discharge was the first method available for the production of both multiwall nanotubes (MWNTs) [17,18] and singlewall nanotubes (SWNTs) [19,20]. It is worth noting that this technique has been in use for a long time for the production of carbon fibers and that it is very probable that nanotubes were observed before 1991 but not recognized as such [21,22]. MWNTs produced by arc discharge are long and straight tubes closed at both ends with graphitic walls running parallel to the tube axis.

An arc discharge with a cathode containing metal catalyst (such as cobalt, iron or nickel) mixed with graphite powder results in a deposit containing SWNTs [19,20,23,24]. SWNTs are usually assembled in ropes but some single tubes can also be found in the deposits. Laser ablation is a related method where the graphite–catalyst target is vaporized by a laser [25].

The second group of production methods is based on the decomposition of a hydrocarbon gas over a transition metal. Carbon filaments and fibers have been produced by thermal decomposition of hydrocarbons since the 1960s [26]. Usually, a catalyst is necessary to promote growth [27]. In general, the catalytic growth yields nanotubes of larger diameter as compared to the arc discharge, along with a crystalline structure that is not perfectly graphitic. For the production of MWNTs, acetylene is usually used as the carbon source at temperatures typically between 600

and 800 °C. To grow SWNTs the temperature has to be significantly higher (900–1200 °C) and carbon monoxide or methane is used.

3.2. Vaporization methods

Nanotube films can be realized from the raw or purified material obtained with vaporization methods in several ways. For example, a colloidal suspension of material can be drawn through a nanopore alumina filter and the resulting film can then be transferred by pressing the filter face-down on a Teflon or Teflon-coated metal surface [10,28–30]. Spraying the suspension on a heated substrate yields similar results [31].

An alternative is to disperse the tubes in a matrix. The first experiments with colloidal graphite were described in 1994, but no field emission could be observed [32,33]. Positive results were obtained by using nonconducting epoxies [34] or other products [35,36].

One important prerequisite to using carbon nanotubes as electron emitters in some microelectronic devices is to be able to apply them in patterns onto the substrate. This can be achieved with nanotubes produced by vaporization methods, and indeed the first field emission displays were realized by mechanically pressing a nanotube/epoxy paste into channels etched in a glass substrate (Fig. 2a) [37–39]. The surface of the cathode is then polished to expose the channels after curing. Similar methods involve the deposition of carbon nanotubes from a solution [40–42]. It seems, however, that an activation step (e.g., by plasma etching [39]) is necessary to obtain field emission. Furthermore, the method is not adapted to incorporate nanotube emitters in gated structures.

3.3. CVD methods

The CVD methods are ideally suited to grow films of nanotubes on planar substrates such as silicon [43–47] or glass [48,49]. Several techniques have been demonstrated in the past years. Thermal CVD is a simple pyrolysis, usually performed in a flow reactor inside a tubular oven. The CVD process can also be assisted by a hot filament and/or by a microwave or rf plasma. The latter two embodiments are more complicated but allow a significant decrease of the growth temperature [50]. There are several reasons behind the development of catalytic techniques to grow carbon nanotubes on planar substrates. In many cases, there are no or very few codeposited carbon allotropes. Cumbersome purification steps are thus unnecessary. Finally, since the growth is activated by a catalyst, the deposition of catalyst at predefined locations followed by catalytic growth will result in substrates patterned with nanotubes.

One possibility is to use standard lithographic techniques, such as photolithography or e-beam lithography. Basically, a resist is coated on the substrate, exposed and developed, creating a pattern of resist on the surface as shown in Fig. 2b. The resist pattern can be used as a mask to deposit the catalyst on the unprotected part of the substrate, thereby creating a negative of the resist pattern [51]. Conversely, the resist pattern can be used as a protection when the catalyst is evaporated on the surface

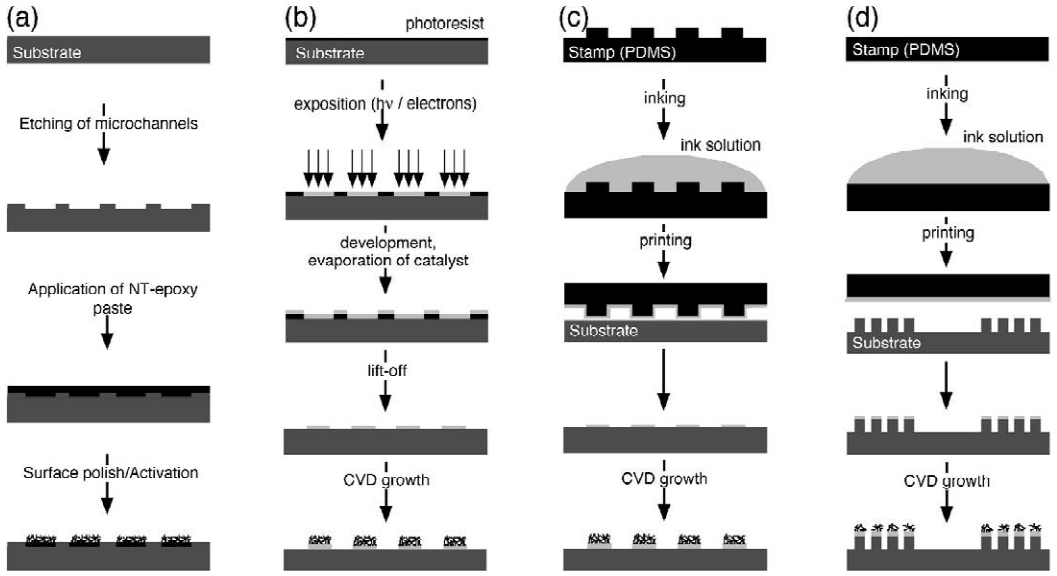

Fig. 2. Techniques to produce patterned films of carbon nanotubes: (a) squeeze-paste; (b) standard lithography followed by CVD growth; (c) soft lithography with a structured stamp on a flat substrate followed by CVD growth; (d) soft lithography with a flat stamp on a structured substrate followed by CVD growth.

prior to the patterning, and the unprotected catalyst is removed with an acid or by plasma etching [52]. The resist is then removed by a solvent. A related method is shadow masking, where the catalyst is deposited on the substrate (or where the nanotubes are grown) through a mask that is in contact with the substrate (e.g., a physical object like a TEM grid) [43,53,54].

A second possibility is to use non-photolithographic techniques such as soft lithography [55,56]. The common feature of all variations of soft lithography is a patterned elastomer (the 'stamp') that permits a spatially controlled delivery of material to a surface. For the patterned growth of nanotubes, microcontact printing (μCP, which is one variation of soft lithography) of catalyst precursors has been successfully implemented as shown schematically in Fig. 2c [46,57]. The structured stamp, obtained by curing an elastomer over photoresist patterns defined on a Si wafer (the 'master'), is loaded with a catalyst solution (the 'ink'). The catalyst is then transferred onto the substrate by mechanical contact [46]. This allows great flexibility with the catalyst: since the ink is a solution, one can vary the composition and concentration of dissolved transition metal salts. In addition, the process is not based on the use of expensive equipment necessary to perform standard lithography. A similar approach using μCP has been presented using a flat stamp to transfer the catalyst onto a substrate consisting of regularly patterned silicon towers, as shown in Fig. 2d [58,59].

4. Field emission from nanotube films

4.1. Overview

It is now established that nanotubes were produced and studied before Iijima identified them in 1991 [21,22], and this also certainly applies to field emission studies. Nevertheless, we usually consider that the first studies on electron emission from carbon nanotubes were published in 1995 [28,60,61]. Their potential was immediately apparent, as extremely low turn-on fields [28] and high current densities [28,61] were reported. Only a few studies followed during the next two years. From 1998 on, the perspective to use nanotubes as field emission devices spurred efforts worldwide: a first display [37] as well as a lighting element were presented [62].

Most reports on field emission describe the fabrication method of the film emitter and present a typical *I–V* curve. Basically, all studies show that field emission is excellent for nearly all types of nanotubes. Field emission is observed at macroscopic fields as low as 1 V/μm, and turn-on fields are typically around 5 V/μm (the turn-on field is the macroscopic field needed to extract a current density of 10 $\mu A/cm^2$). Nanotube films are capable of emitting current densities up to a few A/cm^2 at fields below 10 V/μm. Two tables summarizing the results obtained can be found in Ref. [8].

One of the problems in comparing results obtained by different groups is that the methods used for synthesis (SWNTs, MWNTs), purification (closed or open ends, presence of contaminating material), and film deposition (alignment, spacing between the tubes) are quite varied. The interpretation is further complicated by the different experimental setups, e.g. the use of planar, spherical or sharp tip anodes, and different inter-electrode distances. It therefore seems necessary in a first stage to discuss results acquired on different nanotube films under the same experimental conditions. It then appears that several parameters have an impact on the emission. First, the intrinsic structural and chemical properties of the individual tubes play a role, as marked differences were found depending on the diameter [10] and surface treatment [63] as well as between closed and open tubes [10]. Second, the density and orientation of the tubes on the film [10,31,64] also influence the emission. Comparison and interpretation of the results is difficult because most groups either use different experimental procedures, vary several parameters or do not completely characterize their samples. It is hence unclear whether the observed variations in field emission properties are due to different intrinsic properties of the tubes (e.g., SWNTs as compared to MWNTs) or to the preparation method. To underscore this point, we observed a slightly inferior emission for SWNTs than for randomly aligned MWNTs [10], while Bower et al. measured the inverse behavior for SWNTs and densely aligned MWNTs [31].

4.2. Influence of the film morphology on the field emission

To address this problem, we present in the following sections two detailed examples, which will illustrate the influence of the morphology of the film emitters. The results underline that the growth conditions have to be carefully controlled in order to to optimize the emission and to ensure reproducible characteristics.

The field emission was characterized at a base pressure of 10^{-7} mbar by collecting the emitted electrons with a polished stainless steel spherical counterelectrode of 1 cm diameter, which corresponds to an emission area of 0.007 cm^2 according to electrostatic calculations. The samples were mounted on a linear manipulator, and the inter-electrode distance d_0 was adjusted to 125 μm prior to emission. It was decreased to 50 and finally 10 μm when no field emitted current was detected below 1100 V applied voltage. The field amplification factor β was obtained by fitting the *I–V* curves at low emitted currents with the Fowler–Nordheim formula using a workfunction of 5 eV, which is a reasonable assumption for carbon-based field emitters.

4.2.1. Tuning the film morphology with the catalyst

In a first series of experiments, we used microcontact printing (μCP) to pattern Si substrates with catalyst solutions of different concentrations (1 to 50 mM $Fe(NO_3)_3 \cdot 9H_2O$ in ethanol). The deposition of MWNTs was carried out in a standard CVD flow reactor at 720 °C [46,65,66]. It turns out that varying the concentration of catalyst in the solution influences directly the density of MWNTs on the patterned film, as illustrated in Fig. 3 [46,65,66]. When the concentration is increased from 1 to 40 mM, we observe an increase of the density of the deposited nanotubes. For low concentrations (1 mM, Fig. 3a) only a few single nanotubes are distributed randomly over the printed zones. Increasing the concentration of the catalyst is accompanied by the formation of a film of entangled nanotubes as shown in Fig. 3b for 40 mM. Finally, a concentration around 50 mM results in arrays of nanotubes aligned perpendicular to the surface, similar to aligned assemblies of nanotubes found by other groups [43,48,67]. As displayed in Fig. 3c, the side walls are flat and no tubes are branching away. For concentrations higher than 60 mM the growth of nanotubes is almost inhibited and the pattern is decorated by carbon particles.

On all samples a stable field emission was measured

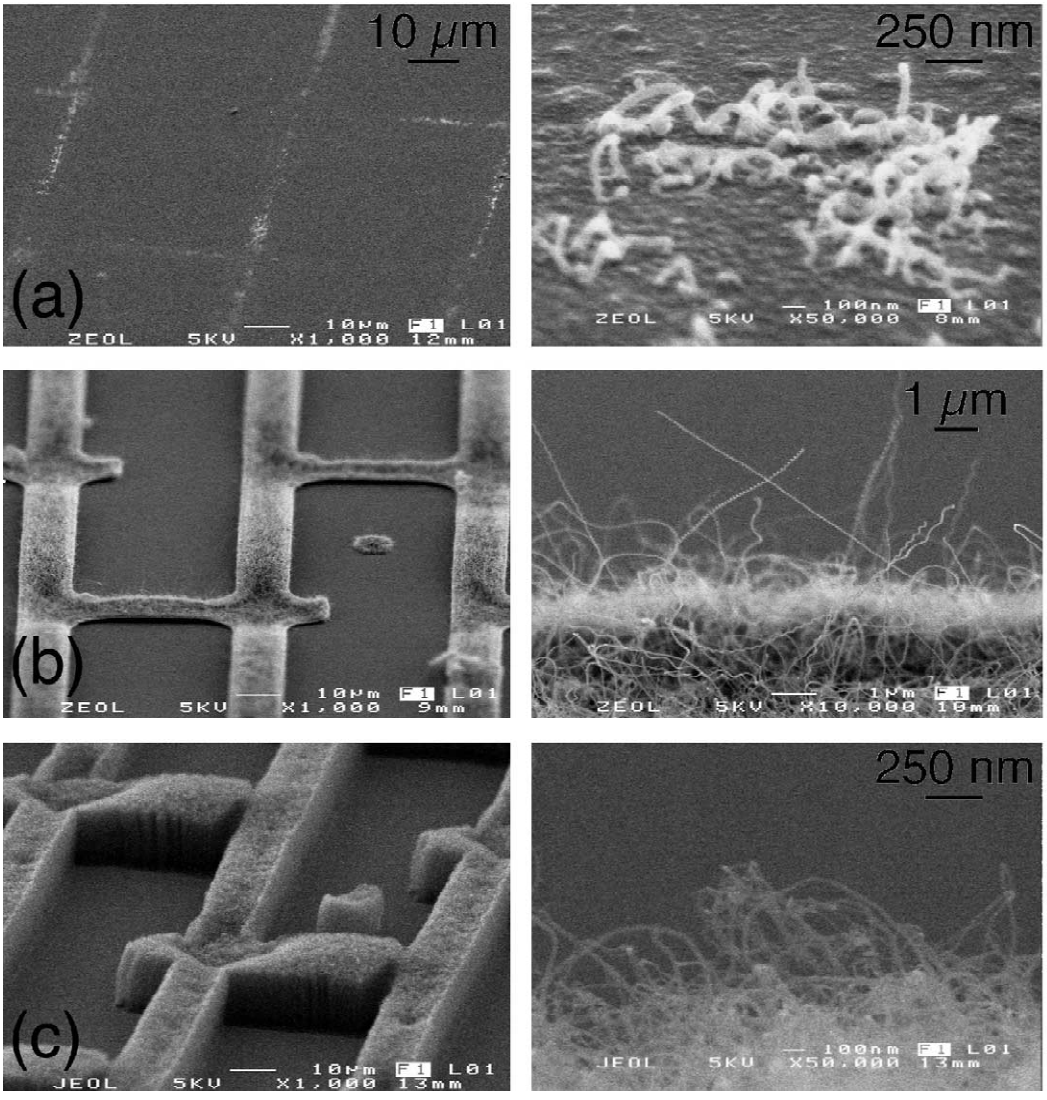

Fig. 3. Scanning electron microscopy (SEM) micrographs at a grazing incidence of 20° to the substrate of patterned MWNT films realized by μCP and ink with different catalyst concentrations. The magnification of the micrographs in the right column is 10× (b) and 50× (a,c) higher than in the left column. (a) Low, (b) medium, and (c) high nanotube density corresponding to concentrations of 1, 40 and 50 mM, respectively.

during the first voltage ramp. We found, however, that the application of high currents degraded the emission [66]: an example is shown in Fig. 4a. The left curve corresponds to the emission of the pristine film and could be reproduced as long as the field remained below 1.3 V/μm, i.e. the highest field applied so far. The extraction of higher currents invariably resulted in a degradation of the emission that showed up as a shift of the *I–V* curve towards higher fields. This degradation also involved a decrease in the field amplification. We believe that this phenomenon involves some kind of 'training' process where the best but mechanically or electrically fragile emitters are damaged or destroyed. One possibility to circumvent this problem is to systematically operate the emitters at 30 mA/cm^2 for 30 min to ensure reproducible characteristics up to 10 mA/cm^2. In the case of Fig. 4a this corresponded to an applied macroscopic electric field of 4.4 V/μm, and the *I–V* curve on the right in Fig. 4a is characteristic of the sample after training.

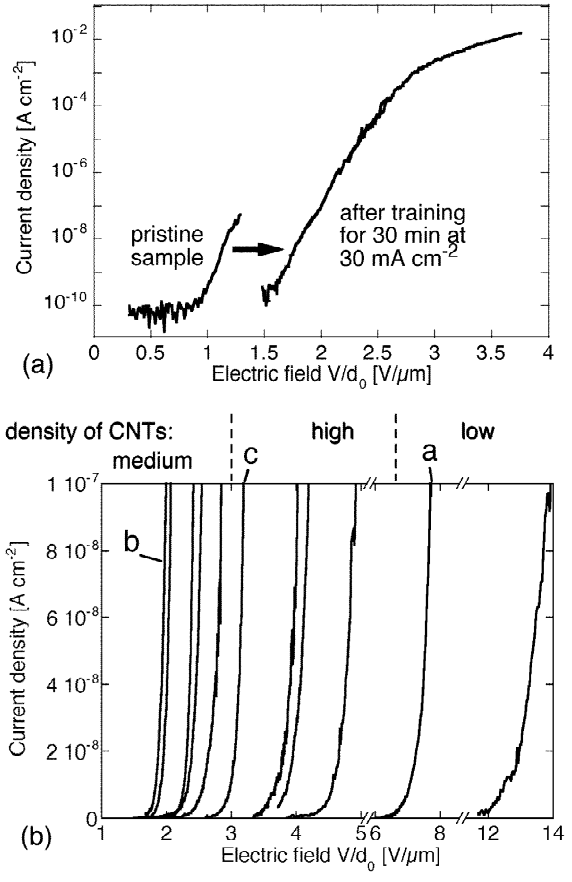

Fig. 4. (a) Field emission characteristics of a film of medium density similar to that shown in Fig. 3b before and after the training step. (b) Low current field emission characteristics of the 11 samples after training. The curves acquired on the films depicted in Fig. 3 are indicated.

The analysis of samples of different densities proved that films of medium densities with nanotubes protruding over the film surface show emission at the lowest fields [66] (see Figs. 3b and 4b). Field emission is measured below 2.5 V/μm, and they reach 10 mA/cm^2 below 4.5 V/μm, which puts them among the best nanotube field emitters [8]. Films of lower and higher density follow at higher fields (e.g., the film shown in Fig. 3c). All these samples emit consistently below 5 V/μm and have threshold fields below 10 V/μm. The low density films (Fig. 3a) need far higher applied fields.

These results are shown in Fig. 5, where the field amplification factor β is plotted against the onset field E_i, which is the macroscopic electric field V/d_0 needed to extract 10 nA/cm^2. The samples with the lowest onset fields also show the highest field amplification. Conversely, the low density films required much higher E_i. To extract some quantitative information from Fig. 5, we make the assumptions that the emitter density is identical for all samples, that all MWNTs have the same workfunction, and that all MWNTs on one given sample have the same field amplification factor. In that case, each emitter has to supply the same current for a given current density regardless of the density and geometrical characteristics of the films. It follows from the Fowler–Nordheim model that the local field at the emitter tip $F = \beta V/d_0$ has to be the same for every emitting tube. One obtains in the case of Fig. 5 that $\beta = F/(V/d_0) = F/E_i$, i.e. the field amplification varies as the inverse of the onset field with the local field at the emitter surface as the only parameter. We have fitted the experimental points in Fig. 5 with this formula and obtained a local field at the emitter tip of 2.6±0.1 V/nm. This is quite remarkable, because this value obtained from measurements on 11 different samples corresponds well to

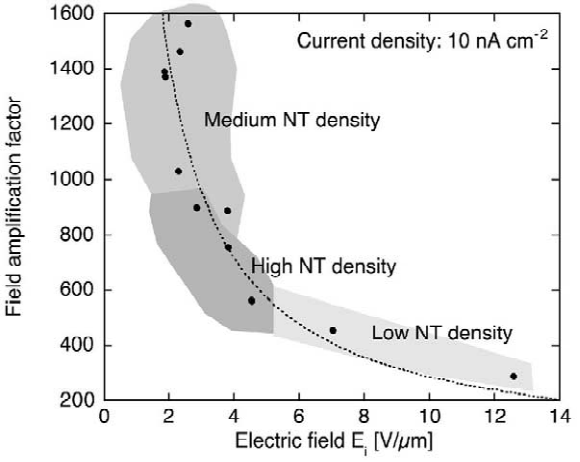

Fig. 5. Field amplification factor β as a function of the onset field after training, E_i, for the films obtained by CVD with different catalyst concentrations (Figs. 3 and 4). The dotted curve represents the best fit to the formula $\beta = F/E_i$ with $F = 2.6 \pm 0.1$ V/nm.

the local field needed to initiate field emission on one emitter. It has to be noted that this result does not validate the above assumptions. In particular, the emitter density probably varies significantly from sample to sample, but its influence is minimized by the highly non-linear increase of emitted current with the applied field: a variation of the emitted current of an order of magnitude coincides with a change of 7% only in the applied field, as can be extracted from Fig. 4.

The emission was also characterized on a microscopic scale with a vacuum scanning FE apparatus that uses a scanning tip to locally resolve field emission [68]. The low density samples showed a rather inhomogeneous emission pattern with very few sites emitting a low current. A much more homogenous emission image is obtained for a medium density. The samples of high density yielded a result similar to the low density sample, albeit with an emission intensity higher by a factor of 10. We argue in Section 4.2.3 that these differences arise mostly from geometrical and morphological considerations.

4.2.2. Tuning the film morphology with the deposition conditions

Recently, the possibility of growing nitrogenated carbon (C:N) nanotubes with up to 4% N was demonstrated by decomposition of CH_4 in a N_2 and NH_3 atmosphere with a bias-enhanced hot filament CVD technique [69,70]. When only one resistively heated WC filament is used, the overall distance between filament and substrate varies with the lateral distance *x*. This provokes a gradual variation of the deposition conditions, as the temperature, composition and flux of the gas mixture as well as the temperature of the substrate T_{sub} depend on the distance to the filament. For example, T_{sub} was found to decrease from 780 °C directly underneath the filament down to 690 °C at large distances [71,72].

We used μCP to transfer an ethanolic ink containing 60 mM $Fe(NO_3)_3 \cdot 9H_2O$ and 20 mM $Ni(NO_3)_2 \cdot 6H_2O$ to the Si substrate, and MWNTs were deposited by hot filament CVD [71,72]. TEM also reveals that thin needle-like structures protrude from the surface of the tubes [71]. A catalyst particle of complex shape and covered with a few graphitic sheets is present at the tip of the nanotubes [72]. SEM pictures of the resulting structures are shown in Fig. 6a–d. The diameter of the nanotubes is found to vary between 30 nm and 1 μm as a function of *x* (see also Fig. 8a). The thickest tubes are found directly underneath the filament (Fig. 6a). The diameter then decreased with increasing *x* (Fig. 6b) down to ~50 nm for $x = 5$ mm (Fig. 6c). For larger distances, we found a further decrease in diameter for some tubes while other tubes showed an increase in diameter, resulting in a wide dispersion (see Fig. 6d for $x = 10$ mm).

The field emission was measured at various locations on the film between $x = 0$ and 20 mm, and Fig. 7 shows a strong variation in the field emission characteristics. Directly underneath the filament ($x \leq 1$ mm), the inter-electrode distance had to be reduced to 10 μm to observe field emission below 1100 V. As *x* increased, the fields needed for emission decreased rapidly (see Figs. 7 and 8b), and reached a minimum for $x = 5$ mm. The emission fields again increased, and levelled off for distances larger than $x = 8$ mm. We found that a current density of 10 mA/cm^2 could be reached repeatedly at every measured location, and that the emission was stable with time.

To analyze the results in more detail, we extracted several parameters from the *I–V* characteristics of Fig. 7 and displayed them in Fig. 8 as a function of the lateral distance *x*. The field amplification is given in Fig. 8c, and Fig. 8b shows the onset field E_i. To correlate these parameters with the film morphology, the tube diameter as estimated by SEM is given in Fig. 8a. Fig. 8 reveals that the field emission properties of the C:N nanotube film vary over a large range and clearly depend on the lateral distance *x*, and hence on the deposition conditions. The very high emission fields measured directly underneath the filament coincide with a large tube diameter and a correspondingly low field amplification. We then observe a spectacular correlation between these three parameters: as the mean diameter decreases sharply, the emission fields decrease drastically with a corresponding increase in field amplification. The lowest fields were achieved at $x = 5$ mm, corresponding to temperatures between 730 and 750 °C and tube diameters of ~50 nm. The morphology of the film becomes more complex for larger *x*, as two nanotube populations appear, one showing a further decrease in diameter down to 30 nm, and the other characterized by a slow increase followed by a saturation around $x = 15$ mm to diameters of ~150 nm (Fig. 8b). Interestingly, the emission fields increase and the field amplification decreases beyond $x = 5$ mm: the tendency does not follow the decrease in diameter of the smaller tube population (lower branch in the upper panel of Fig. 8).

4.2.3. Discussion

On emitter assemblies like those shown in Figs. 3 and 6, only the nanotubes with the highest field amplification will emit, which in turn means that the actual emitter density is lower than the nanotube density by as much as several orders of magnitude. We may hence readily understand that a film of low density and short tubes (e.g., that depicted in Fig. 3a) will be an inefficient cathode. We have noted that the medium density films obtained by CVD (Fig. 3b) show a very homogeneous and strong emission with a large number of emitting sites. A very dense film (Fig. 3c), however, shows a decreased quality of emission. This results from a combination of two effects: the inter-tube distance and the number of emitters. When the inter-tube distance is large, the field amplification factor is determined only by the diameter and the height of the nanotube. As the distance between the tubes is decreased, screening effects become significant. Since the density of

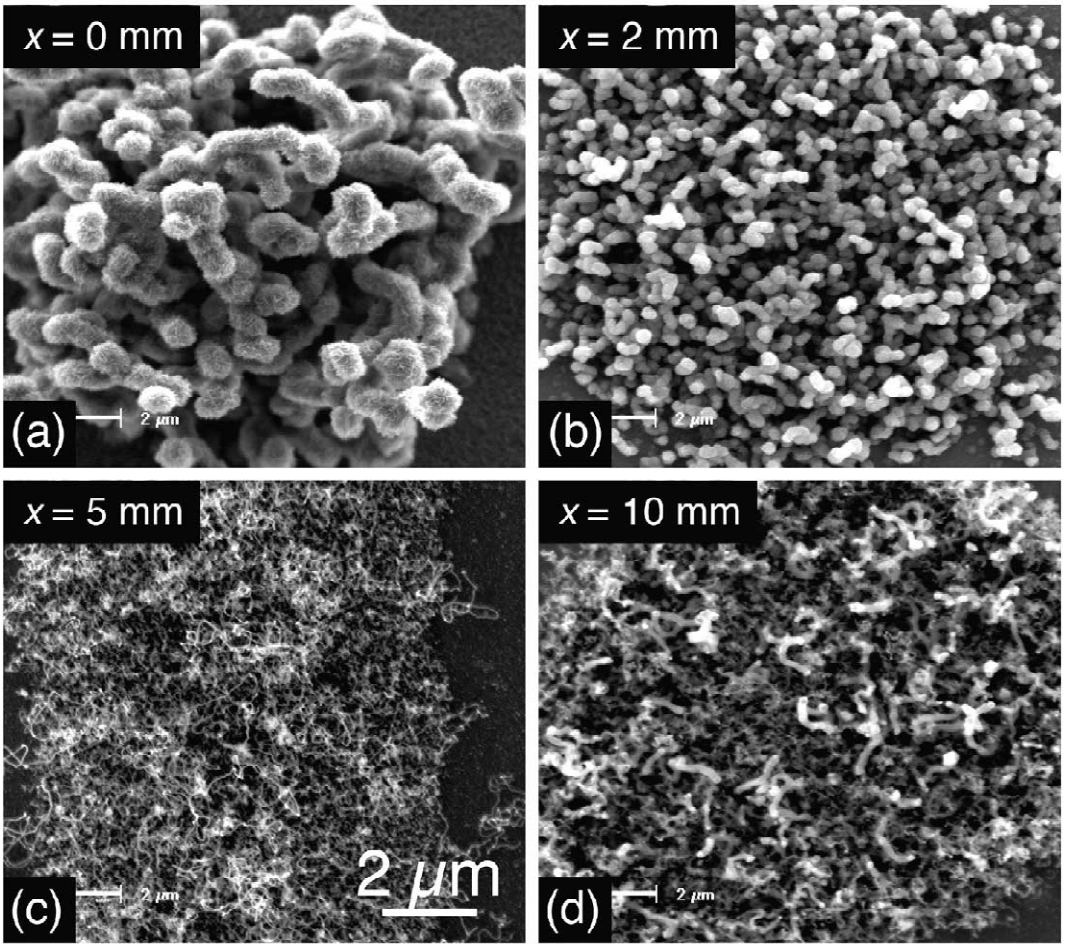

Fig. 6. (a) SEM micrographs showing the dependence of the film morphology C:N nanotubes grown by HF-CVD as a function of the lateral distance to the filament x: (a) $x = 0$ mm; (b) $x = 2$ mm; (c) $x = 5$ mm; (d) $x = 10$ mm.

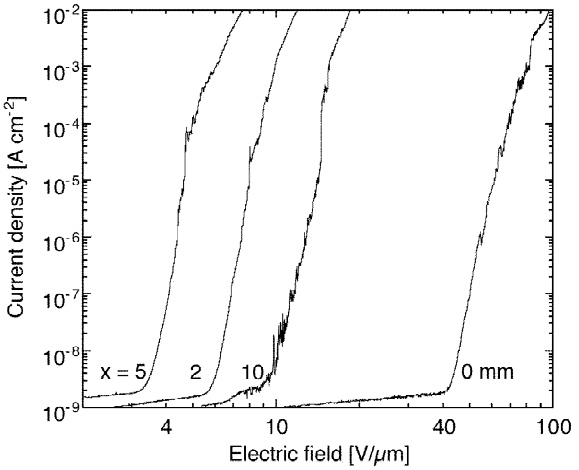

Fig. 7. Field emission I–V characteristics taken at different lateral distances x corresponding to the SEM micrographs of Fig. 6. The applied field is given as the macroscopic field V/d_0 at the cathode surface.

emitters increases with decreasing inter-tube distance, there will be an optimum distance for a maximal emitted current density. Electrostatic calculations indicate that this distance amounts to one to two times the tube height [68]. The height of the tubes over the substrate (or the average film surface) is of course another important parameter [68]. In fact, the influence from the substrate—or from the average film surface—is significant even for long tubes. Our three CVD samples of Fig. 3 correspond, therefore, to three different emission regimes. The turn-on fields for low density films are high because there are few emitters with short heights. Conversely, the emission from high density films is more efficient but remains low because of screening effects between densely packed neighboring tubes and because of the small height of the tubes. There is an ideal compromise between these two extremes, where the length of the tubes and the distance between neighboring emitters are both sufficient to reach a high field amplification along with an emitter density that is high enough to ensure homogeneous emission at low voltages.

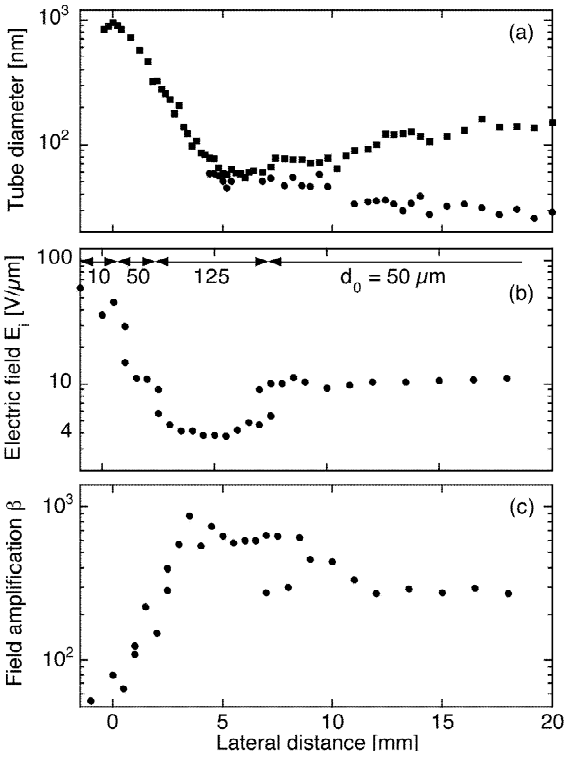

Fig. 8. Structural and field emission parameters as a function of the lateral distance x corresponding to the SEM micrographs of Fig. 6. (a) Mean tube diameter as estimated by SEM. (b) Onset field E_i (the inter-electrode distance d_0 is also indicated). (c) Field amplification factor β. The spreads in the fields and β from one measurement to the next are typically ±5% and ±15%, respectively.

The results obtained for the films of Fig. 6 show an additional influence. As the field emission is critically influenced by the field amplification, one could suppose that a film with nanotubes of small diameter will necessarily be more efficient as compared to a film with nanotubes of larger diameter, since the former incorporates more efficient emitters. However, Fig. 8 reveals that the field emission is not governed solely by the diameter of the smallest tubes. If this were the case, the emission fields should decrease further for $x > 5$ mm, as the diameter of the smaller tubes decreases down to ~30 nm. This confirms that the field amplification is not given only by the geometrical shape of the emitting nanotubes. In the case of Fig. 6d, the smaller tubes (i.e., the most probable emitters) are surrounded by higher and thicker tubular structures which screen the applied field and decrease the actual field amplification.

These two examples demonstrate clearly that the field amplification of a film emitter is determined by both the geometrical shape of the emitters and their surroundings, as the presence of nearby objects screens the applied electric field and provokes a decrease in the effective field amplification. This shows again the necessity of controlling precisely the morphology of the film to optimize the emission properties.

4.3. Degradation of nanotube films

For any future application, the prerequisite for the long-term stability of the emitting films must be fulfilled. The degradation of the emission is usually due to several phenomena and can be either reversible or permanent. Irreversible damage can occur through resistive heating, bombardment from gas molecules ionized by the emitted electrons, or arcing. Electrostatic deflection or mechanical stresses can cause alterations in the shape and/or surroundings of the emitter and lead to a decrease of the local field amplification. Other degradation phenomena are of chemical origin (adsorption or desorption of molecules on the emitter surface) and modify the workfunction.

The longest test to-date has been performed by Saito et al., who report an increase of 11% of the applied field to maintain an emission current of 10 mA/cm^2 for 8000 h [36]. Other studies show, nevertheless, that degradation can occur on shorter time scales.

At present, the origin of degradation is not clear. It seems that residual gases have a significant influence [38,73] and that the emitted current density is also important [10,74]. In addition, the intrinsic properties of nanotubes also have an importance. A comparison between films of SWNTs and MWNTs at comparable chamber pressure and emitted current density showed that the degradation was a factor of 10 faster for SWNTs [10,30]. The faster degradation of SWNTs was attributed to the fact that their single shell makes them more sensitive to ion bombardment and irradiation, while the multiple shells of MWNTs tend to stabilize their structure.

Finally, the configuration used for emission (parallel plates or plan-to-sphere configurations with distances of 100 μm, or field emission microscope setups with far larger inter-electrode distances) may also play a role. Dean et al. suggested that the poor vacuum conductance between two closely placed planes leads to high local pressures of gases like water or oxygen that cause reactive etching and hence faster degradation [75]. This may also be of importance in a display environment and will warrant some additional precautions.

4.4. Outlook

The two examples presented above show that it is possible (a) to pattern substrates with nanotubes and (b) to control to some extent the morphology of the films either through the catalyst or the deposition conditions. This allows a systematic optimization of the field emission properties of the films, and hence the reproducible realization of homogeneous films emitting at low applied fields.

Another concern is the deposition temperature. The CVD was performed at 720 °C for the films shown in Fig.

3, and the temperature at the substrate surface reached 780 °C during the hot filament CVD process for the film shown in Fig. 6. The temperature has to be decreased below 650 °C for display applications, which is the upper limit for glass substrates. However, MWNTs have been grown below this limit with hot filament and/or plasma-enhanced CVD [48,49]. We also recently showed that MWNTs can be obtained by simple thermal CVD between 630 and 650 °C by optimizing the catalyst, on Si [76] as well as glass [77] substrates.

Two points still remain open in spite of their utmost importance for applications. The first is the controlled incorporation of nanotube emitters in gated structures, which is a prerequisite for a display. Nothing prevents this incorporation in principle, but several technological hurdles will have to be addressed. The second, the effective emitter site density, is a big unknown. We know that nanotube films emit low fields but we do not know how many of them actually emit. A film has a typical nanotube density of 10^8–10^9 cm^{-2}. Densities of 10^3–10^4 cm^{-2} were reported at the onset of emission [28,73,74,78], which is too low by at least one order of magnitude for a display. A systematic optimization has therefore to be undertaken to reach higher emitter densities while keeping low emission fields.

5. Field emission applications

Applications based on nanotube film emitters are diverse. Nanotube flat-panel displays were proposed in 1995 as an enticing alternative to other film emitters [28,60], and it took only three years until the first display with 32×32 matrix-addressable pixels in diode configuration was realized by Wang et al. [37]. The Samsung group demonstrated a fully sealed 4.5 inch three color field-emission display in 1999 [38,39] and has progressed rapidly to 4.5 inch full-color images and 9 inch full color display with 576×242 pixels [79]. As indicated in Section 3, there are numerous technological hurdles related to the deposition of nanotubes in gated structures. Problems such as display sealing, phosphor lifetime, and charging of spacers are further concerns.

Other devices simpler than flat-panel displays have been demonstrated and there are probably many more under investigation. One possibility is to use nanotubes in lighting elements, i.e. to produce light by bombarding a phosphor-coated surface with electrons. Such a cathode-ray tube (also called a 'jumbotron lamp') has been developed by Saito et al. and is commercially available [35]. The brightness is typically higher by a factor of 2 as compared to conventional thermoionic lighting elements, with demonstrated lifetimes of 8000 h [36,49]. Let us mention that the firm that produces these tubes (Ise Electronics, Mie, Japan [80]) has received the silver medal of the 'Displays of the Year Awards 2000' of the Society for Information Display, for their ''high brightness carbon nanotube luminescent elements—the first commercial product that uses field emission from carbon nanotubes''.

Field emitters are also of great interest for microwave amplification [81]. This type of application is very demanding because the current density must be at least 0.1 A/cm^2. Zhou et al. constructed a prototype based on a SWNT cathode that is able to reach that lower limit to operate in microwave tubes [82]. The same group realized a gas discharge tube that serves as an overvoltage protection [83]. When the voltage between a nanotube cathode and a counterelectrode reaches a threshold value for field emission, the emitted current induces a discharge in the noble gas-filled inter-electrode gap. It could be demonstrated that this device shows better performance than commercially available elements.

There have also been attempts to realize lighting elements with field emitters to offer an alternative to incandescent or fluorescent lamps. Such an element could be similar to the cylindrical device depicted in Fig. 9a, where the phosphor layer on the inner surface of the anode is bombarded with energetic electrons emitted by the cathode. To ensure a uniform light emission from the phosphor, the cathode itself must be cylindrical, and the problem of depositing field emitters on a non-planar surface has thus far prevented the realization of such devices.

We were able to obtain uniform cylindrical MWNT cathodes by CVD of acetylene [84]. As we have seen in Section 3, this method was initially optimized for deposition on planar substrates, but nothing prevents the growth of MWNTs on non-planar substrates [85]. We used Kanthal wires (an Fe–Al–Cr alloy) as supports with the same catalytic ink as for Si substrates.

Fig. 10 shows SEM micrographs of a typical cathode. The deposit is homogeneous along the whole length and circumference of the support. Transmission electron microscopy reveals that the tube walls are well graphitized with graphene sheets running approximately parallel to the tube axis with some defects on the tube walls, which is typical of MWNTs grown by catalytic techniques.

For field emission, the supports were mounted in the center of a cylindrical aluminum anode of 21 mm radius and 5 cm length. Fig. 11 shows an *I–V* curve of a typical emitter: the cathode emits a current density of 1 mA/cm^2 for an applied voltage of 1.1 kV, which is quite exceptional for a film emitter placed 2 cm away from the counterelectrode. One has to realize that the cylindrical geometry has a huge advantage over the planar arrangement, as it provides a preamplification of the field due to the difference in radii of curvature between anode and cathode [84]. This makes the realization of a field emission diode working at voltages below a kV possible, provided that one is capable of depositing emitters on a non-planar surface.

We show in Fig. 9b a luminescent tube realized with a cylindrical MWNT cathode. The anode is an ITO-coated

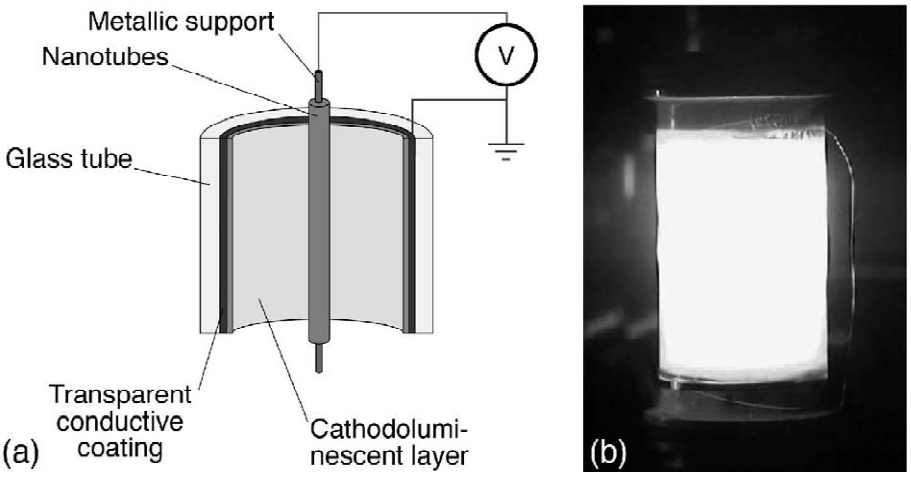

Fig. 9. (a) Luminescent field emission device in cylindrical geometry: the conductive cathode supports the emitters and is placed on the symmetry axis of the cylindrical anode. The anode is a glass tube with a conductive coating and a phosphor layer on the inner surface. (b) Luminescent tube realized with a MWNT cathode. The applied voltage was 7.5 kV, the emitted current density 0.25 mA/cm^2 on the cathode and 0.03 mA/cm^2 on the anode. The emitted light intensity amounts to 10^4 cd/m^2.

glass tube with a phosphor layer (Lumilux B45) on the inner surface, and serves both as vacuum enclosure and as light producing element. The applied voltage used in Fig. 9 amounts to 7.5 kV to ensure a reasonable phosphor efficiency, yielding an emitted current density of 0.25 mA/cm^2 on the cathode and 0.03 mA/cm^2 on the anode (this corresponds to the maximal output of our high tension power supply). The luminence of the tube under these conditions is 10^4 cd/m^2 as measured with a photometer, and is comparable to a commercial fluorescent tube (11 000 cd/m^2). The power needed for operation is at the moment significantly higher than for a fluorescent tube. This difference is mainly due to the efficiency of the phosphor. The white phosphor used here has an efficiency of 10 lm/W only, as compared to the typical 70 lm/W for a white fluorescent tube.

Although only a laboratory prototype, the device shown in Fig. 9 represents an enticing alternative to usual fluorescent tubes, as it contains no mercury, starts up instantly, and is readily dimmable. Furthermore, the use of cylindrical MWNT cathodes is not restricted to lighting elements. They can be implemented in any application where a high current in a cylindrical geometry is needed, such as vacuum gauges or magnetic field sensors.

All these achievements underline the potential of carbon nanotube emitters in applications. Nevertheless, the lack of information on some aspects of device realization, such as device lifetime, fabrication yield and cost, show the demand for more studies. It remains, however, that tremendous progress has been achieved during the last years, and that we can expect answers to these open questions in the near future.

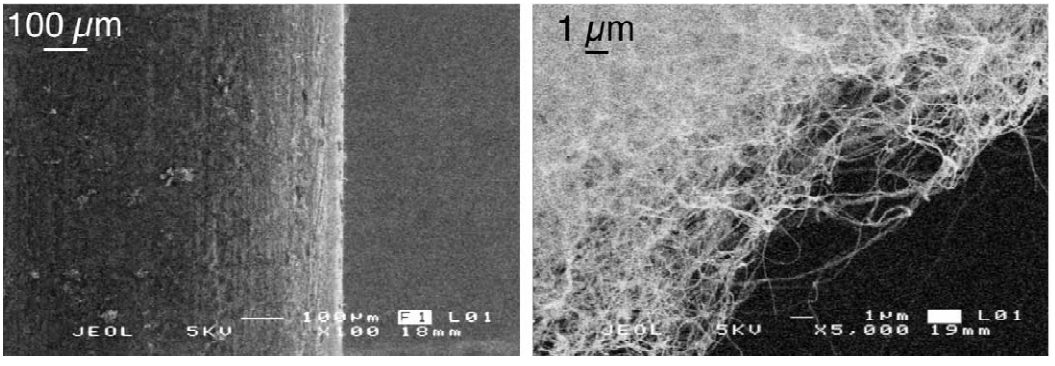

Fig. 10. SEM micrographs of a typical cylindrical MWNT field emission cathode.

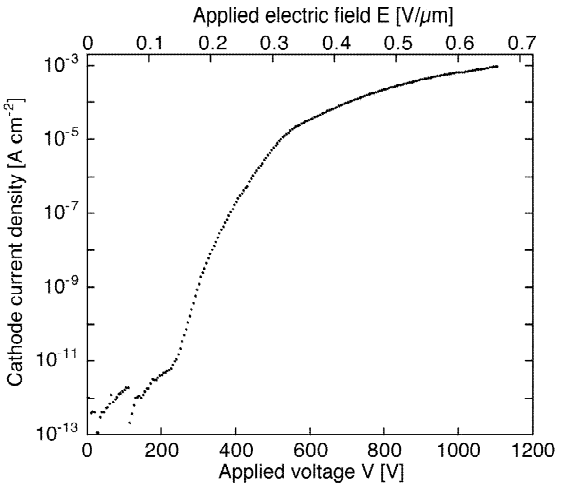

Fig. 11. (a) *I–V* curve for the MWNT cathode displayed in Fig. 10. The applied field is given as the macroscopic field at the cathode surface.

6. Conclusion

As was apparent from the very beginning, nanotubes are excellent electron sources operating at low emission fields, providing a stable current and capable of operating in moderate vacuum. There are now methods at our disposal for depositing various types of nanotubes on surfaces. Various techniques have been developed to pattern the films and define pixels on the cathodes, to vary the density of nanotubes or their orientation on the deposit, and to vary their morphology with the deposition conditions. This makes it possible to control and optimize their emission properties.

There remain, however, numerous gaps in our understanding, especially on the fundamental aspects. These gaps will only be bridged through detailed studies and comparative experiments where great care is taken to control the physical and chemical state of the emitters. Related questions such as the problem of electrical contacts to nanotubes will have to be addressed. Degradation also remains a large unknown in spite of its utmost importance for applications. The optimization of the emitter density, which is still poorly characterized, as well as the incorporation of nanotubes in gated devices, are also important milestones for the evolution of the field.

It remains, however, that tremendous progress has been achieved in the past years. With devices as varied as flat panel displays, microwave tubes and lighting elements based on carbon nanotube emitters, and (probably) with additional applications in the making, we can confidently state that carbon nanotube emitters are promised a bright future.

Acknowledgements

The work presented here was performed in close collaboration with the members of our group. André Chatelain, László Forró, Klara Hernadi (visiting from the University of Szeged, Hungary), Ayatollah Karimi, Klaus Kern, and Hannes Kind all participated in the film preparation, CVD growth, structuring of nanotube films, and in the various studies on field emission. We gratefully acknowledge their precious contributions. The electron microscopy was performed at the Centre Interdépartemental de Microscopie Electronique of EPFL. Financial support was provided by the Swiss National Science Foundation, the TopNANO21 program, NanoLight International Ltd. and the European project CANADIS.

References

[1] Dresselhaus MS, Dresselhaus G, Eklund PC. Science of fullerenes and carbon nanotubes. New York: Academic Press, 1996.
[2] Ebbesen TW. Carbon nanotubes: preparation and properties. Boca Raton: CRC Press, 1997.
[3] Harris PJF. Carbon nanotubes and related structures—new materials for the twenty-first century. Cambridge: Cambridge University Press, 1999.
[4] Ebbesen TW. Carbon nanotubes. Phys Today 1996;49(6):26–32.
[5] Ajayan PM, Ebbesen TW. Nanometre-size tubes of carbon. Rep Prog Phys 1997;60(10):1025–62.
[6] Dekker C. Carbon nanotubes as molecular quantum wires. Phys Today 1999;52(5):22–8.
[7] Rao CNR. Carbon nanotubes. Chem Phys Chem 2001;2:78.
[8] Bonard JM, Kind H, Stöckli T, Nilsson LO. Field emission from carbon nanotubes: the first five years. Solid State Electron 2001;45:893.
[9] Schmid H, Fink HW. Carbon nanotubes are coherent electron sources. Appl Phys Lett 1997;70(20):2679–80.
[10] Bonard JM, Salvetat JP, Stöckli T, Forró L, Châtelain A. Field emission from carbon nanotubes: perspectives for applications and clues to the emission mechanism. Appl Phys A 1999;69(3):245–54.
[11] Good RH, Müller EW. Field emission. Handbuch der Physik 1956;21:176.
[12] Dyke WP, Dolan WW. Adv Electron Electron Phys 1956;8:89.
[13] Gadzuk JW, Plummer EW. Rev Mod Phys 1973;45:487.
[14] Gomer R. Field emission, field ionization, and field desorption. Surf Sci 1994;299/300:129–52.
[15] Forbes RG. Refining the application of Fowler–Nordheim theory. Ultramicroscopy 1999;79(1–4):11–23.
[16] Adessi C, Devel M. Theoretical study of field emission by single-wall carbon nanotubes. Phys Rev B 2000;62(20):R13314–7.
[17] Iijima S. Helical microtubules of graphitic carbon. Nature 1991;354:56–8.

[18] Ebbesen TW, Ajayan PM. Large-scale synthesis of carbon nanotubes. Nature 1992;358(6383):220–2.
[19] Iijima S, Ichihashi T. Single-shell carbon nanotubes of 1-nm diameter. Nature 1993;363(6430):603–15.
[20] Bethune DS, Kiang CH, de Vries MS, Gorman G, Savoy R, Vazquez J et al. Cobalt-catalysed growth of carbon nanotubes with single-atomic-layer walls. Nature 1993;363(6430):605–7.
[21] Abrahamson J, Wiles PG, Rhoades BL. Structure of carbon fibres found on carbon arc anodes. Carbon 1999;37:1874, originally published in 1979.
[22] Thrower PA. Editorial. Carbon 1999;37:1677.
[23] Maser WK, Lambert JM, Ajayan PM, Stephan O, Bernier P. Role of Y–Ni–B mixtures in the formation of carbon nanotubes and encapsulation into carbon clusters. Synth Met 1996;77(1–3).
[24] Journet C, Bernier P. Production of carbon nanotubes. Appl Phys A 1998;67(1):1–9.
[25] Thess A, Lee R, Nikolaev P, Dai H, Petit P, Robert J et al. Crystalline ropes of metallic carbon nanotubes. Science 1996;273(5274):483–7.
[26] Walker PL, Rakszawski JF, Imperial GR. J Phys Chem 1959;63:133.
[27] Kim MS, Rodriguez NM, Baker RTK. J Catal 1991;131:60.
[28] Heer W, Châtelain A, Ugarte D. A carbon nanotube field-emission electron source. Science 1995;270(5239):1179–80.
[29] Heer W, Bacsa WS, Châtelain A, Gerfin T, Baker RH, Forró L et al. Aligned carbon nanotube films: production and optical and electronic properties. Science 1995;268(5212):845–7.
[30] Bonard JM, Salvetat JP, Stöckli T, Heer W, Forró L, Châtelain A. Field emission from single-wall carbon nanotube films. Appl Phys Lett 1998;73(7):918–20.
[31] Bower C, Zhou O, Zhu W, Ramirez AG, Kochanski GP, Jin S. Fabrication and field emission properties of carbon nanotube cathodes. Mater Res Soc Symp Proc (in press).
[32] Fishbine BH, Miglionico CJ, Hackett KE, Hendricks KJ. Graphene nanotubule cold field emission electron sources. Mater Res Soc Symp Proc 1994;349:319.
[33] Fishbine BH, Miglionico CJ, Hackett KE, Hendricks KJ, Wang XK, Chang RPH et al. Buckytube cold field emitter array cathode experiments. Mater Res Soc Symp Proc 1995;359:319.
[34] Collins PG, Zettl A. A simple and robust electron beam source from carbon nanotubes. Appl Phys Lett 1996;69(13):1969–71.
[35] Saito Y, Uemura S, Hamaguchi K. Cathode ray tube lighting elements with carbon nanotube field emitters. Jpn J Appl Phys 1998;37:L346–8.
[36] Saito Y, Uemura S. Field emission from carbon nanotubes and its application to electron sources. Carbon 2000;38:169.
[37] Wang QH, Setlur AA, Lauerhaas JM, Dai JY, Seelig EW, Chang RPH. A nanotube-based field-emission flat panel display. Appl Phys Lett 1998;72(22):2912–3.
[38] Choi WB, Chung DS, Kang JH, Kim HY, Jin YW, Han IT et al. Fully sealed, high-brightness carbon-nanotube field-emission display. Appl Phys Lett 1999;75(20):3129–31.
[39] Chung DS, Choi WB, Kang JH, Kim HY, Han IT, Park YS et al. Field emission from 45 in single-walled and multiwalled carbon nanotube films. J Vac Sci Technol B 2000;18:1054.
[40] Ahlskog M, Seynaeve E, Vullers RJM, van Haesendonck C. A microdeposition technique for carbon nanotubes based on electron beam lithography. J Appl Phys 1999;85(12):8432–5.
[41] Burghard M, Duesberg G, Philipp G, Muster J, Roth S. Controlled adsorption of carbon nanotubes on chemically modified electrode arrays. Adv Mater 1998;10(8):584.
[42] Liu J, Casavant MJ, Cox M, Walters DA, Boul P, Wei L et al. Controlled deposition of individual single-walled carbon nanotubes on chemically functionalized templates. Chem Phys Lett 1999;303(1/2).
[43] Fan S, Chapline MG, Franklin NR, Tombler TW, Cassell AM, Dai H. Self-oriented regular arrays of carbon nanotubes and their field emission properties. Science 1999;283(5401):512–4.
[44] Lee CJ, Kim DW, Lee TJ, Choi YC, Park YS, Lee YH et al. Synthesis of aligned carbon nanotubes using thermal chemical vapor deposition. Chem Phys Lett 1999;312(5/6).
[45] Araki H, Kajii H, Yoshino K. Growth of carbon nanotubes on quartz plates by chemical vapor deposition using (Ni,Fe)-phthalocyanines. Jpn J Appl Phys 1999;38:L836–8.
[46] Kind H, Bonard JM, Emmenegger C, Nilsson LO, Hernadi K, Maillard-Schaller E et al. Patterned films of carbon nanotubes using microcontact printing of catalysts. Adv Mater 1999;11:1285.
[47] Choi YC, Bae DJ, Lee YH, Lee BS, Han IT, Choi WB et al. Low temperature synthesis of carbon nanotubes by microwave plasma-enhanced chemical vapor deposition. Synth Met 2000;108:159.
[48] Ren ZF, Huang ZP, Xu JW, Wang JH, Bush P, Siegal MP et al. Synthesis of large arrays of well-aligned carbon nanotubes on glass. Science 1998;282(5391):1105–7.
[49] Murakami H, Hirakawa M, Tanaka C, Yamakawa H. Field emission from well-aligned, patterned, carbon nanotube emitters. Appl Phys Lett 2000;76(13):1776.
[50] Chen Y, Shaw DT, Guo L. Field emission of different oriented carbon nanotubes. Appl Phys Lett 2000;76(17):2469–71.
[51] Kong J, Cassell AM, Dai H. Chemical vapor deposition of methane for single-walled carbon nanotubes. Chem Phys Lett 1998;292:567.
[52] Xu X, Brandes GR. A method for fabricating large-area, patterned, carbon nanotube field emitters. Appl Phys Lett 1999;74(17):2549–51.
[53] Yang Y, Huang S, He H, Mau AWH, Dai L. Patterned growth of well-aligned carbon nanotubes: a photolithographic approach. J Am Chem Soc 1999;121:10832–3.
[54] Huang S, Dai L, Mau AWH. Patterned growth and contact transfer of well-aligned carbon nanotube films. J Phys Chem B 1999;103(21):4223–7.
[55] Kumar A, Whitesides GM. Features of gold having micrometer to centimeter dimensions can be formed through a combination of stamping with an elastomeric stamp and an alkanethiol ‘ink’ followed by chemical etching. Appl Phys Lett 1993;63(14):2002.
[56] Xia Y, Whitesides GM. Soft lithography. Angew Chem Int Ed 1998;37:550–75.
[57] Cassell AM, Raymakers JA, Kong J, Dai H. Large scale CVD synthesis of single-walled carbon nanotubes. J Phys Chem B 1999;103(31):6484–92.

[58] Cassell AM, Franklin NR, Tombler TW, Chan EM, Han J, Dai H. Directed growth of free-standing single-walled carbon nanotubes. J Am Chem Soc 1999;121:7975.
[59] Dai H, Kong J, Zhou C, Franklin N, Tombler T, Cassell A et al. Controlled chemical routes to nanotube architectures, physics, and devices. J Phys Chem B 1999;103:11246–55.
[60] Chernozatonskii LA, Gulyaev YV, Kosakovskaya ZY, Sinitsyn NI, Torgashov GV, Yu FZ et al. Electron field emission from nanofilament carbon films. Chem Phys Lett 1995;233:263.
[61] Rinzler AG, Hafner JH, Nikolaev P, Lou L, Kim SG, Tomanek D et al. Unraveling nanotubes: field emission from an atomic wire. Science 1995;269(5230):1550–3.
[62] Saito Y, Hamaguchi K, Uemura S, Uchida K, Tasaka Y, Ikazaki F et al. Field emission from multi-walled carbon nanotubes and its application to electron tubes. Appl Phys A 1998;67(1):95–100.
[63] Dimitrijevic S, Withers JC, Mammana VP, Monteiro OR, Ager III JW, Brown IG. Electron emission from films of carbon nanotubes and Ta–C coated nanotubes. Appl Phys Lett 1999;75(17):2680–2.
[64] Davydov DN, Sattari PA, AlMawlawi D, Osika A, Haslett L, Moskovits M. Field emitters based on porous aluminum oxide templates. J Appl Phys 1999;86(7):3983–7.
[65] Kind H, Bonard JM, Forró L, Kern K, Hernadi K, Nilsson LO et al. Printing gel-like catalysts for the directed growth of multiwall carbon nanotubes. Langmuir 2000;16:6877.
[66] Bonard JM, Weiss N, Kind H, Stöckli T, Forró L, Kern K et al. Tuning the field emission from carbon nanotube films. Adv Mater 2001;13:184.
[67] Terrones M, Grobert N, Olivares J, Zhang JP, Terrones H, Kordatos K et al. Controlled production of aligned-nanotube bundles. Nature 1997;388(6637):52–5.
[68] Nilsson L, Gröning O, Emmenegger C, Küttel O, Schaller E, Schlapbach L et al. Scanning field emission from structured carbon nanotube films. Appl Phys Lett 2000;76:2071.
[69] Kurt R, Karimi A, Hoffman V. Growth of decorated carbon nanotubes. Chem Phys Lett 2001;335:545–52.
[70] Kurt R, Karimi A. Chem Phys Chem 2001;6:388.
[71] Kurt R, Klinke C, Bonard JM, Kern K, Karimi A. Tailoring the diameter of decorated CN nanotubes by temperature variations using HF-CVD. Carbon 2001;39:2163.
[72] Bonard JM, Kurt R, Klinke C. Correlation between deposition conditions and field emission properties of patterned nitrogenated carbon nanotube films. Chem Phys Lett 2001;343:21.
[73] Bonard JM, Maier F, Stöckli T, Châtelain A, Heer W, Salvetat JP et al. Field emission properties of multiwalled carbon nanotubes. Ultramicroscopy 1998;73:9–18.
[74] Zhu W, Bower C, Zhou O, Kochanski G, Jin S. Large current density from carbon nanotube field emitters. Appl Phys Lett 1999;75(6):873–5.
[75] Dean KA, Chalamala BR. The environmental stability of field emission from single-walled carbon nanotubes. Appl Phys Lett 1999;75(19):3017–9.
[76] Klinke C, Bonard JM, Kern K. Surf Sci 2001;492:195.
[77] Klinke C, Bonard JM, Kern K. AIP Conf Proc 2001;591:293.
[78] Küttel OM, Gröning O, Emmenegger C, Nilsson L, Maillard E, Diederich L et al. Field emission from diamond, diamond-like and nanostructured carbon films. Carbon 1999;37(5):745–52.
[79] Kim JM, Lee NS, Choi WB, Jung JE, Han IT, Jung DS et al. 9 inch carbon nanotube-based color field emission displays for large area and color applications. In: Presented at the 14th International Winterschool on Electronic Properties of Novel Materials (IWEPNM2000), Kirchberg, Austria, 2000.
[80] See also http://wwwitron-isecojp/english/nano/indexhtm.
[81] Jensen KL. Field emitter arrays for plasma and microwave source applications. Phys Plasma 1999;6(5):2241.
[82] Zhou O (UNC, Chapel Hill), Zhu W (Lucent Technologies). Pending US patents.
[83] Rosen R, Simendinger W, Debbault C, Shimoda H, Fleming L, Stoner B et al. Application of carbon nanotubes as electrodes in gas discharge tubes. Appl Phys Lett 2000;76(13):1663–6.
[84] Bonard JM, Stöckli T, Noury O, Chatelain A. Field emission from cylindrical carbon nanotube cathodes: possibilities for luminescent tubes. Appl Phys Lett 2001;78:2775.
[85] Bower CA, Zhou O, Wei Z, Werder DJ, Sungho J. Nucleation and growth of carbon nanotubes by microwave plasma chemical vapor deposition. Appl Phys Lett 2000;77(17):2767–9.